Analyst

PAPER

View Article Online
View Journal | View Issue

Cite this: *Analyst*, 2023, **148**, 2141

Monitoring bacterial spore metabolic activity using heavy water-induced Raman peak evolution†

Rasmus Öberg, [a] Tobias Dahlberg,[a] Dmitry Malyshev *[a] and Magnus Andersson *[a,b]

Endospore-forming bacteria are associated with food spoilage, food poisoning, and infection in hospitals. Therefore, methods to monitor spore metabolic activity and verify sterilization are of great interest. However, current methods for tracking metabolic activity are time-consuming and resource intensive. This work investigates isotope labeling and Raman microscopy as a low-cost rapid alternative. Specifically, we monitor the Raman spectrum of enterotoxic *B. cereus* spores undergoing germination and cell division in D_2O-infused broth. During germination and cell division, water is metabolized and deuterium from the broth is incorporated into proteins and lipids, resulting in the appearance of a Raman peak related to C–D bonds at 2190 cm^{-1}. We find that a significant C–D peak appears after 2 h of incubation at 37 °C. Further, we found that the peak appearance coincides with the observed first cell division indicating little metabolic activity during germination. Lastly, the germination and cell growth rate of spores were not affected by adding 30% heavy water to the broth. This shows the potential for real-time monitoring of metabolic activity from a bacterial spore to a dividing cell. In conclusion, our work proposes tracking the evolution of the C–D Raman peak in spores incubated with D_2O-infused broth as an effective and time-, and cost-efficient method to monitor the outgrowth of a spore population, simultaneously allowing us to track for how long the bacteria have grown and divided.

Received 16th December 2022,
Accepted 4th April 2023

DOI: 10.1039/d2an02047e

rsc.li/analyst

1. Introduction

Bacterial spores are a metabolically dormant form of bacteria that are very resilient to natural deterioration and decontamination methods such as heat, cold, electromagnetic radiation, and chemical treatment.[1,2] Under favourable conditions, however, spores germinate (turn back into metabolically active vegetative cells) and start dividing. Because of their inherent resilience, pathogenic spore-forming bacterial strains cause problems in food production, healthcare, and homeland security.[3–5]

To understand the mechanisms behind spore resilience, and evaluate spore response to chemicals, robust methods for monitoring spore metabolic activity are needed. Cell metabolomics can be used to exactly identify particular metabolites,[6,7] but this method is very time-, and resource intensive and requires making mutant strains of the studied bacterial species.[6] Fluorescent dyes such as DAPI can be used to monitor the viability of cells and spores, however, they can be toxic to cells in the process.[8] Also, monitoring metabolic activity is of importance in decontamination and spore viability determination as spores that appear "dead" may, in fact, be viable and merely have delayed or disrupted germination and therefore fully recover in the presence of nutrients.[9] Conversely, a spore may be able to germinate but be non-viable and unable to proceed to cell division.[10] Currently, the most widespread technique to determine spore viability is culture growth on agar plates with rich media,[11,12] which is a very robust but time-consuming process needing 48 hours of incubation for clinically relevant species like *C. difficile*.[13] Furthermore, tracking spore metabolic activity during outgrowth is important in understanding germination and growth rate in different environments.

A novel method for tracking the metabolic activity of microorganisms has recently emerged, utilizing deuterium oxide and micro-Raman spectroscopy. Deuterium oxide (D_2O), also called heavy water, is a heavier isotopic form of water with its hydrogen atoms replaced with deuterium. The additional neutron in deuterium compared to its single proton counterpart results in different chemical and physical properties in D_2O compared to H_2O.[14] The heavier weight of the deuterium atoms shifts the vibrational frequencies of formed bonds involving deuterium, compared to hydrogen.[15] If H_2O is switched to D_2O during cell growth, deuterium is incorporated into the cell through metabolic reactions such as the $NADP^+$ redox reac-

[a]*Department of Physics, Umeå University, 901 87 Umeå, Sweden.*
E-mail: dmitry.malyshev@umu.se, magnus.andersson@umu.se
[b]*Umeå Centre for Microbial Research (UCMR), Umeå, Sweden*

† Electronic supplementary information (ESI) available. See DOI: https://doi.org/10.1039/d2an02047e

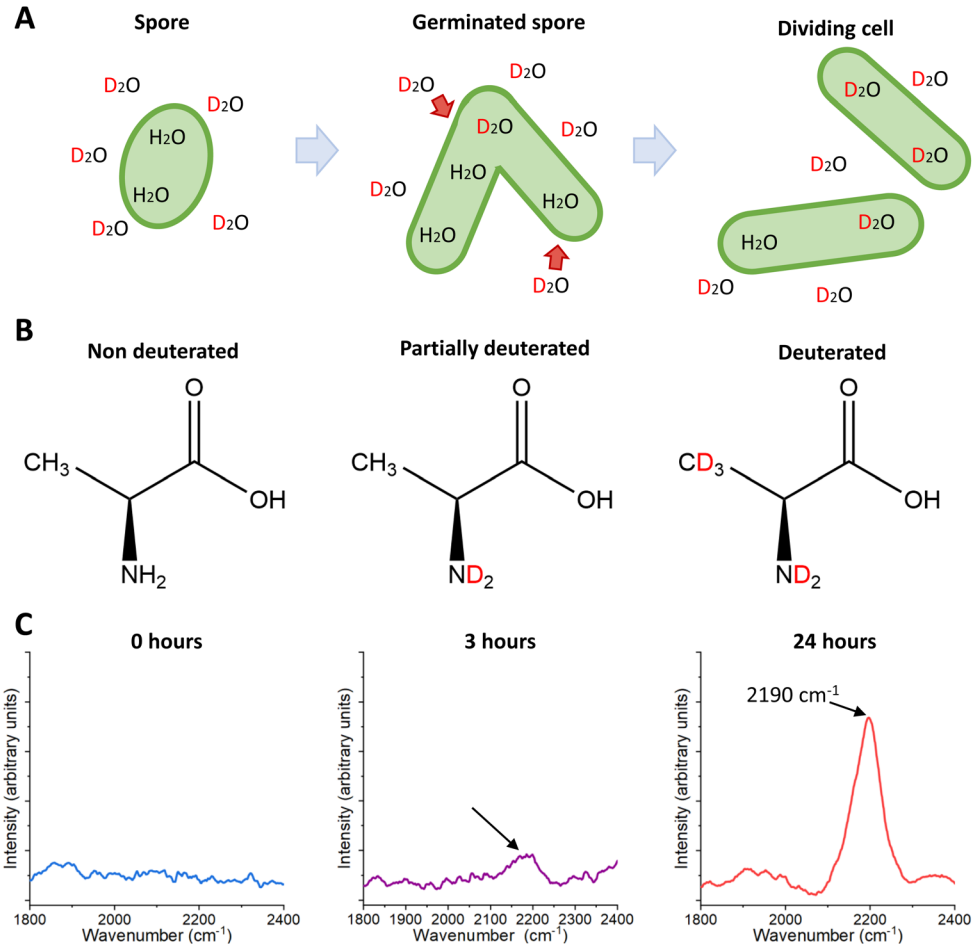

Fig. 1 Uptake of deuterium in D_2O by spore forming bacteria. (A) A spore starts largely dehydrated, with no D_2O. As it germinates and proceeds to cell division, D_2O is taken up by the cells. These cells incorporate deuterium into their amino acids, such as alanine (B), replacing the hydrogen isotope. (C) The resulting C–D bond has a characteristic band in the 2100–2300 range, centered at ~2190 cm^{-1}, that increases in peak area over time in growing bacterial cultures.

tions resulting in a H–D exchange during, for example, acetyl-CoA fatty acid synthesis. Deuterium thereby accumulates in the cell as it is incorporated into proteins and lipids with the C–D bonds replacing the C–H bonds (Fig. 1A and B).[16] These C–D bonds express a broad Raman band around 2190 cm^{-1}, an otherwise quiet spectral region, allowing for easy quantification of the Raman band. Therefore, the incorporation of D_2O in the growth medium enables the assessment of cellular metabolic activity at the individual cell level using Raman spectroscopy as demonstrated by previous studies[16–18] and as illustrated in Fig. 1C.

This technique presents an advantage in screening for viable cells, as it can identify seemingly inactivated cells, as long as they are still metabolically capable.[19] Previous studies have utilized the characteristic Raman bands from C–D bonds to study, among other things, cell activity, antimicrobial susceptibility, and cancer cell detection.[16,20–22] However, this technique has not yet been applied to spores, raising the question of whether it can be used to monitor the metabolic activity of spores' germination and growth.

In this paper, we present an evaluation of the potential of micro-Raman spectroscopy using C–D vibrational bands to determine and quantify spore germination and growth. We utilize a laser tweezer Raman setup to monitor the appearance and intensity development of D_2O-induced Raman peaks of *B. cereus* spores at approximately 2190 cm^{-1}. Our study aims to determine the point after germination when metabolism can be detected by monitoring individual spores during their germination and initial divisions. Additionally, we assess the potential toxic effect of D_2O to ensure that D_2O does not impact spore germination and growth at the utilized concentrations.[23]

2. Materials and methods

2.1. Raman- and absorption spectroscopy systems

To acquire Raman spectra from single spores, we use a laser tweezer Raman spectroscopy (LTRS) setup (Fig. S1†) built around an inverted microscope (IX71, Olympus), described in

greater detail in previous works.[24,25] We couple a 785 nm Gaussian laser beam with a maximum power of 120 mW (08-NLD, Cobolt) into our microscope system using a dichroic short pass mirror with cut-off wavelength of 650 nm (DMSP650, Thorlabs). We focus the beam using a 60× water immersion objective with a numerical aperture of 1.2 (UPlanSApo, Olympus) and working distance of 0.28 mm. To gather Raman spectra, we collect the backscattered light through the microscope objective. Rayleigh scattered light is filtered out using a 785 nm notch filter (NF785-33, Thorlabs) and then filtered using a 150 μm diameter pinhole in the focal point of the telescope. The light is then coupled into a spectrometer (Model 207, McPherson) and dispersed using its 600 grooves per mm holographic grating with an 800 nm blaze. Lastly, the Raman spectra are captured with a Peltier cooled CCD detector (Newton 920N-BR-DDXW-RECR, Andor) operated at −95 °C and we use Solis (Solis v4.30, Andor) software to control the detector and acquire spectra. The spectral resolution of our instrument is <3 cm^{-1}. Optical microscopy images were taken using PH3 phase contrast and using a 100×, numerical aperture 1.35 oil immersion objective (UPlanApo, Olympus).

We acquire the optical density of bacterial suspensions using the absorption module of a UV-VIS spectrophotometer (Lambda 1050+, PerkinElmer) by measuring on suspensions in 1 ml polystyrene cuvettes (No. 67.742, Sarstedt).

2.2. Spore strain and stock preparation

We measure Raman spectra on *B. cereus* NVH 0075/95 spores prepared as follows. Spores were prepared on blood agar plates stored at 37 °C for approximately three weeks or until the sporulation rate was 95%. We harvested the spores by scraping them off the agar surface and suspending them in autoclaved distilled water. The spore suspension was washed three times in distilled water (centrifugation at 4500 rpm for 5 minutes). The pellet was resuspended in 20% nycodenz (Axis-Shield) and added to a 50% and 45% (w/v) Nycodenz gradient (1 : 1 v/v ratio) before subjected to centrifugation at 4500 rpm for 45 minutes. The pelleted spores were then washed once, and stored in autoclaved distilled water at 4 °C until use. Before use, the concentration of the spore suspensions was adjusted to 10^6 spores per ml, followed by vortexing at 2800 rpm (VM3 Vortex, M. Zipperer GmBH) for 15 seconds.

2.3. D_2O-substituted growth media preparation

Increased concentration tryptic soy broth stock (icTSB) was prepared by mixing TSB powder (Bacto™, BD) with a reduced amount of water (70 ml instead of 100 ml). We incubate a sample for LTRS by mixing 70 μl of icTSB, 30 μl D_2O, and 2 μl of a 10^6 spores per ml suspension. The spores are then left to incubate at 22 °C or 37 °C (room temperature and optimal growth temperature respectively), depending on the experiment.

2.4. Sample preparation and measurement

We prepare a sample for Raman spectroscopy by taking 1 μl of the previously incubated spore or cell suspension (depending on incubation time) and mixing it with 9 μl deionised water to limit the background signal from the broth. We place the 10 μl drop on a 24 × 60 mm glass coverslip (no. 1, Paul Marienfeld GmbH & Co., Lauda-Königshofen, Germany). We apply a vacuum grease ring (Dow Corning, Midland, MI) around the drop and then place a 20 × 20 mm coverslip (no. 1, Paul Marienfeld GmbH & Co., Lauda-Königshofen, Germany) on top to seal the sample to prevent evaporation. Raman spectra are recorded by trapping a single spore or cell using optical tweezers with a laser power of 60 mW on the sample. We use 10 accumulations of 10 seconds in the spectral range of 1900–2300 cm^{-1} to acquire spectra and carry out measurements on at least 10 individual spores in three separate solutions for each incubation time. Thus, we acquire data from 30 spores for each experiment and the results of this study are based on 30 technical replicates and 3 biological replicates. The laser power and accumulation times result in a total applied energy of ~6 J on the spores, well below the 20 J shown to cause spore damage,[26] with previous studies suggesting extensive laser light exposure may inhibit spore germination and growth *via* generation of reactive oxygen species.[27] We keep the spores trapped at a consistent height of 100 μm above the glass surface to maintain a consistent baseline for the spectra with minimal influence from the coverslip. Furthermore, we acquire a background spectrum of the solution (3 technical replicates) at a height of 100 μm above the glass surface to be used for background subtraction.

To track the Raman signal during germination and early divisions, we use a similar methodology. However, we replace the glass coverslips with two 0.25 mm thick relatively Raman-inactive quartz coverslips (43210 Series, Alfa Aesar) to lower the background signal from the glass. This is necessary as spores/cells must be settled on the surface to maintain visual control of specific spore germination, outgrowth and division. We perform Raman measurements on spores deposited on the surface of the slide. Additionally, to limit noise from the growth media we use a lighter mixture consisting of 60 μl PBS, 10 μl icTSB, 30 μl D_2O, and 2 μl of a 10^6 spores per ml solution. This lighter media further helps Raman measurements by making germination and divisions slower and easier to measure.

We incubate samples for optical density measuring by mixing 700 μl icTSB, 300 μl D_2O/H_2O, and 20 μl of 10^6 spores per ml solution and leaving the samples to incubate in cuvettes at 22 °C and 37 °C. Wemix reference cuvettes containing 70 μl icTSB and 30 μl D_2O/H_2O.

To verify that no Raman peak evolution occurs in inactivated spores we mix 90 μl of spore suspension with 10 μl of 1500 ppm chlorine dioxide (DK-DOX 1500, Dr Küke GmbH.) and leave the mixture for 10 minutes. Chlorine dioxide in the suspension is then neutralised with 0.5% sodium thiosulphate. The inactivated spores are then washed by centrifuging in deionised water, discarding the supernatant, and then incubated in the same way as other spores at 37 °C for 24 hours.

2.5. Data processing and statistical analysis

To process our Raman spectra, we use an open-source Matlab (Matlab2018b, Mathworks) script provided by the Vibrational

Spectroscopy Core Facility at Umeå University.[28] We subtract the background and then baseline-correct the spectra using an asymmetrical least squares algorithm[29] and with the algorithm parameters set to $\lambda = 10^6$ and $p = 10^{-3}$. We then smooth the spectra using Savitzky–Golay filtering[30] (polynomial order 1 and frame rate 45). We evaluate peak intensity by calculating the area under the curve between 2100 and 2300 cm^{-1} on the baseline-corrected spectra.

Statistical data analysis is performed using Prism 9 (Prism 9.3, GraphPad Software). Optical densities were compared using Wilcoxon matched-pairs test. We made an ANOVA test to compare the distribution of the values, followed by the application of Dunn's multiple comparisons test to make comparisons with the control group. Peak deconvolutions were performed using Origin 2020 (OriginLab). Optical density data were fitted to a non-linear curve fit (Boltzmann). We plot our figures using Prism and Origin 2020.

3. Results and discussion

3.1. C–D Raman peak intensity indicates metabolic activity in growing cells

To determine whether the C–D Raman peak at 2190 cm^{-1} can be used to evaluate germination and cell growth, we measure the Raman signal of spores incubated in TSB with 30% D_2O over 24 h at 22 °C. The Raman signal of these spores after incubation shows a significant peak evolution over time as observed in Fig. 2A and B. After 3 h we observe Raman activity significantly higher than spores that were not incubated ($p < 0.05$), and after 24 h the Raman peak has further grown considerably compared to its non-incubated counterpart ($p < 0.0001$). By contrast, control spores incubated in D_2O-infused broth for 24 h at 4 °C, a temperature at which the spores should not germinate, did not show a significant change in their Raman spectra compared to their non-incubated counter-

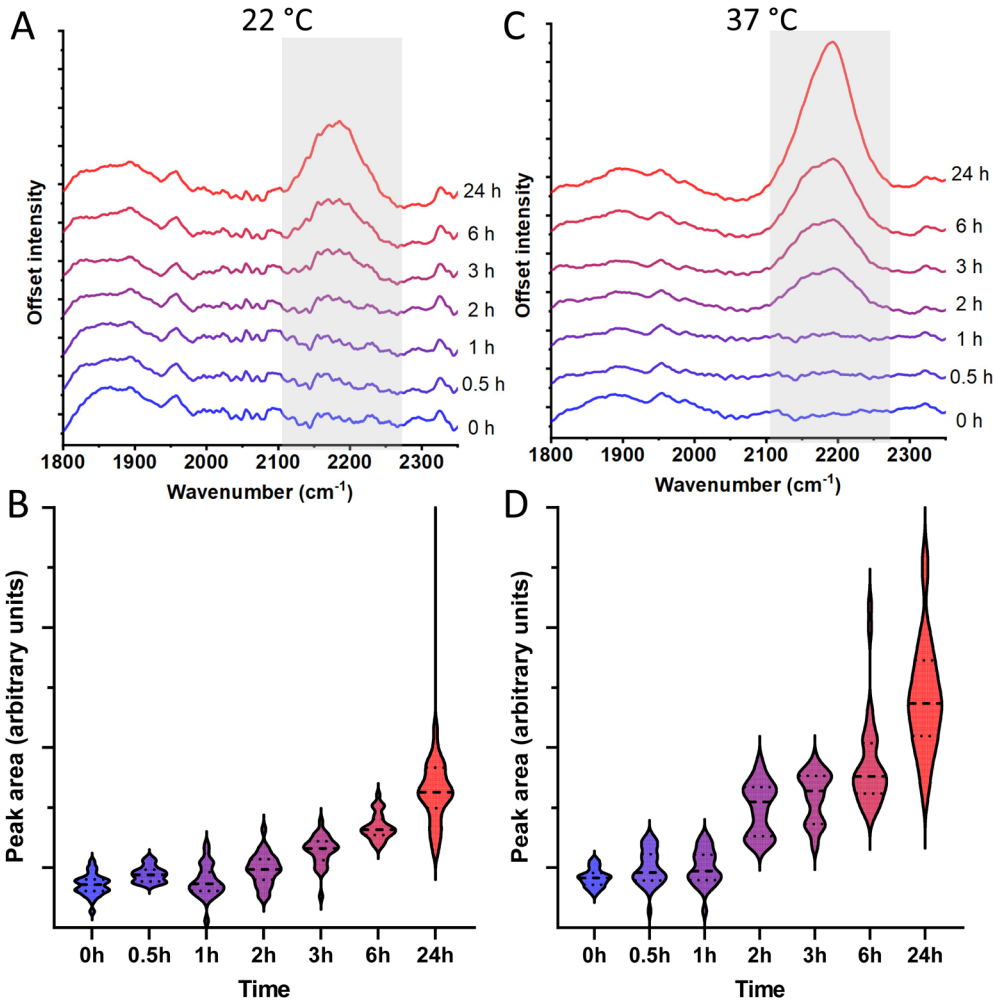

Fig. 2 The evolution of the C–D Raman peak over 24 h for *B. cereus*, incubated at 22 °C and 37 °C (n = 30 for each time point). Each spectrum (A and C) is an average of the 30 spectra for the respective time point. The peak is not present at the start but becomes more prominent over time. The distribution of peak areas between measurements is shown in the violin plots in B and D. The dashed lines show the median and the upper and lower quartiles in the peak area distribution. In both data sets, one cell had a significantly higher peak prominence than all others after 24 hours (outside the shown scale). Other smaller peaks in the spectrum are static and not growing.

part as shown in Fig. S2† (p = 0.41). A peak deconvolution of our data (not shown) suggests that the C–D peak consists of component peaks at 2154, 2198, and 2232 cm^{-1}. These component peaks do not entirely coincide with those reported in works on the C–D peak in other biological contexts.[31] This is expected as relevant proteins and lipids may experience slight differences in Raman frequency in different contexts, as well as the established uncertainty in accurately deconvoluting Raman peaks.[32,33]

To determine whether the Raman peak intensity evolution is proportional to *B. cereus* growth rate, we perform further Raman measurements on spores incubated at 37 °C, a more optimal temperature for growth of *B. cereus*. As seen in Fig. 2C and D, we observe that the Raman peak intensity evolution of spores incubated at 37 °C is faster compared to spores incubated at 22 °C. Statistically significant Raman peak evolution (p < 0.05) compared to the non-incubated spores occurs already after 2 h. Furthermore, after 24 h we observe an increase in Raman intensity almost twice of that observed over the same time span when incubating at 22 °C. This suggests it is possible to use the evolution of the C–D Raman peak to measure whether a spore population has germinated and grown, as well as, how long the germinated spores have been allowed to grow.

To verify that deactivated spores do not display significant C–D Raman activity, we first inactivate spores with 150 ppm chlorine dioxide for 10 minutes and then incubate and measure their Raman signal. As seen in Fig. S3†, we observe no significant peak evolution after 3 h or 24 h implying that no metabolic activity is taking place, as expected from a spore suspension exposed to a high chlorine dioxide concentration known to deactivate spores.[34]

From these results it is clear that the C–D peak from bacterial spores can be used to indicate spore outgrowth and subsequent divisions long before visible colonies would be established using plate growth methods. Compared to the highly

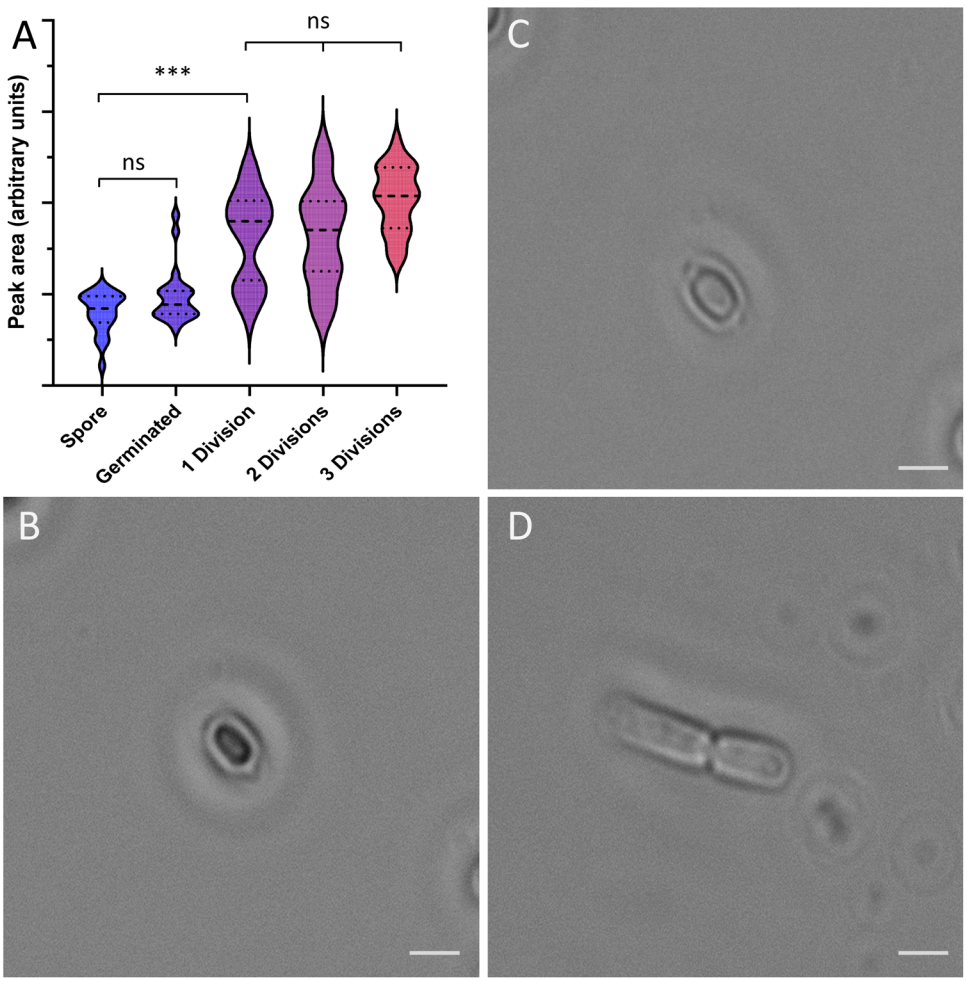

Fig. 3 (A). The area of the C–D Raman peak in *B. cereus*, depending on germination stage (n = 30 for each time point). The dashed lines show the median and the upper and lower quartiles in the distribution. There is no significant difference in peak area between spores (B) and germinated spores (C) (p > 0.99), although there were 2 outlier spores. There was a significant difference between undivided cells and cells that have undergone at least 1 division (D) (p = 0.0003), though there was no significant difference in peak intensities between 1, 2, or 3 divisions (p = 0.62). Panels B–D imaged using bright field and a 60× water immersion objective. Scale bars are 1 μm.

active spectral Raman range of approximately 600–1900 cm^{-1} (Fig. S4†), the C–D peak's position in a quiet Raman region renders it an easily detectable indicator. Compared to older spore germination and outgrowth detection methods that are still in use, C–D peak detection proves to be a convenient alternative. Assays for extracting and detecting calcium dipicolinate (CaDPA) such as those by Janssen *et al.*, and Warth are able to indicate germination within hours, however, the more laborious spore treatments and use of chemicals in these methods may make them inconvenient in many instances.[35,36] Additionally staining methodologies such as the one presented by Hamouda *et al.* are able to detect germination within a few hours.[37] Although rapid, this method has similar drawbacks, and requires staining a spore sample with malachite green as well as safranin-O under high temperatures. As such, the preparation step is somewhat laborious, and may affect the viability of the spore sample by exposing it to genotoxic substances as well as high temperatures.

3.2. Live-tracking spore germination and early cell divisions indicate significant Raman signal alongside first division

To determine the specific stage of spore germination where significant metabolism of D_2O occurs, and thereby an increase in the specific Raman signature, we track the Raman peak evolution of spores as they undergo germination and initial divisions, as shown in Fig. 3A. These measurements are performed using a lighter broth than previous measurements to ensure a high signal-to-noise ratio, as well as to slow down germination and divisions to allow for easier tracking. In the initial spore stage (Fig. 3B), we observe little to no Raman signal from spores in the 2190 cm^{-1} region. We observe little change in the Raman signal as germination takes place, with spores releasing their stored CaDPA and increasing in size (Fig. 3C) compared to their earlier spore form ($p > 0.99$). However, the Raman signal observed from the cells increases during outgrowth and initial divisions (Fig. 3D). Cells that have undergone a single division show a marked increase in peak intensity compared to spores ($p = 0.0003$). Additional divisions with higher incubation time entail further Raman peak intensity evolution as observed in Fig. 2. However, we do not observe a statistically significant increase in the Raman signal between individual divisions past the first division ($p = 0.62$ for the first 3 divisions). This suggests that there is significant D_2O metabolism in the initial cell outgrowth and first division, and that in subsequent divisions the incorporation of deuterium is largely offset by the cell division (and halving of divided cell mass). We also observe a binary distribution in the peak intensities after the first division. We attribute this to the heterogeneity of spore germination, where some spores germinate very quickly, while others germinate after a lag time.[38] Thus, they would be in different stages of the same division cycle, and therefore different amounts of deuterium incorporated.

These results indicate that there occurs very limited or no water-utilising metabolic activity (such as $NADP^+$ or NAD^+ redox reactions) in spore germination stages preceding vegetative cell outgrowth. The results also show that viable spores can be detected as long as they have undergone a single division, even if they re-sporulate later. Metabolic activity can still take place in spores with no visible C–D peak, using the stored energy sources of the spore, such as malate, however, our data precludes any significant biosynthesis of sugars or proteins. This aligns with the detailed metabolic data on spore germination previously reported, where the full metabolic cycle (TCA cycle) only began in the final stage of preceding vegetative cell growth and division.[39] The results highlight the flexibility of using heavy water and Raman spectroscopy to monitor metabolism. We can obtain real-time data on a wild-type isolate with no genetic modification, and we can monitor the metabolism of the sample suspension continuously without using any additional chemicals, and without the bleaching that occurs when using fluorescent dyes. Thus this method presents a low-cost and largely non-invasive way of monitoring metabolism in spore-forming species.

3.3. D_2O does not influence spore germination and growth rate

Previous studies have shown that the presence of D_2O in concentrations of 50% may influence growth and metabolic activity within cells and bacteria.[23,40] To determine whether the presence of D_2O in any way affects the pace at which *B. cereus* spores germinate and grow, we incubate a spore sample in D_2O-infused broth in a cuvette at 37 °C and measure how the optical density at 600 nm (OD_{600}) in the solution develops over time. A higher OD_{600} implies spore outgrowth and divisions, with a larger spore concentration absorb-

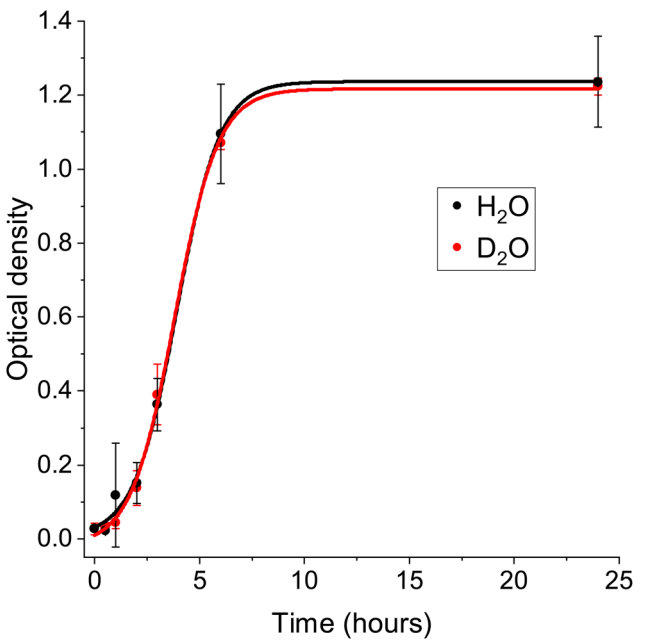

Fig. 4 Optical density of cell suspensions incubated in TSB infused with 30% H_2O (black) compared to TSB infused with 30% D_2O (red), with $n = 3$ for each, fitted with growth curves (Boltzmann). There was no significant difference between the growth curves ($p = 0.47$). Error bars show standard deviation.

ing and scattering more light. We then compare the OD_{600} of the D_2O-infused sample to the OD_{600} of a reference sample replacing the D_2O with H_2O. We observe similar growth in both samples, with an increase in OD_{600} from ~0.02 at the start to ~0.39 after 3 h (Fig. 4). After 24 h we observe an OD_{600} ~1.22 in both samples. Overall there is no statistical difference between the growth curves (p = 0.47). This result is in line with previous works by Zhang *et al.*, following bacterial growth by infusing bacteria with D_2O,[16] however, it also further verifies that the D_2O does not significantly interfere with spore germination and initial outgrowth. Thus, we conclude that our methodology of infusing growth media with 30% D_2O does not affect the germination and growth rate of *B. cereus*, an advantage over fluorescent probes which can be toxic to cells.

4. Conclusions

Spore forming bacteria are problematic in society, and methods to monitor metabolic activity in spores are useful to both understand their biochemistry, and to track their viability and chemical inactivation. Currently there are methods to track spore metabolism, but the ones currently in use are both costly and time-consuming. In this work, we investigate a method utilizing micro-Raman spectroscopy to measure the metabolic activity of spores grown in TSB infused with 30% D_2O. The hypothesis was that when spores metabolise D_2O, a C–D vibrational band will evolve at 2190 cm^{-1} acting as a marker for germination and growth. We found that it is possible to detect a strong C–D peak after only 2 h of incubation at 37 °C, indicating that the metabolic activity was initiated. Furthermore, the data shows significant metabolic activity starting from the first cell division, while the C–D Raman signal immediately after germination remains mostly the same. This suggests that spores do not metabolize large amounts of the surrounding broth-D_2O mixture during germination but rather directly after germination, during the initial outgrowth stage. As a consequence, the C–D peak can be used to monitor metabolic activity already at initial spore outgrowth. Lastly, we found no difference in germination and growth rate between spores incubated with D_2O and H_2O, suggesting no impact from the D_2O on spore germination and growth. Overall, we hope this method will be useful in monitoring spore germination and outgrowth.

Author contributions

Rasmus Öberg: Conceptualization, methodology, investigation, formal analysis, writing – original draft, writing – reviewing and editing. Tobias Dahlberg: Software, resources. Dmitry Malyshev: Conceptualization, methodology, investigation, formal analysis, writing – original draft, writing – reviewing and editing. Magnus Andersson: Methodology, supervision, project administration, funding acquisition, resources, writing – reviewing and editing.

Conflicts of interest

The authors declare no competing financial interest.

Acknowledgements

This work was supported by the Swedish Research Council (2019-04016); the Umeå University Industrial Doctoral School (IDS); Kempestiftelserna (JCK-1916.2); and Swedish Department of Defence, Project no. 470-A400821. We thank Marina Aspholm for providing the *B. cereus* spores.

References

1 G. C. Stewart, The Exosporium Layer of Bacterial Spores: a Connection to the Environment and the Infected Host, *Microbiol. Mol. Biol. Rev.*, 2015, **79**, 437–457.
2 P. Setlow, Spores of *Bacillus subtilis*: Their resistance to and killing by radiation, heat and chemicals, *J. Appl. Microbiol.*, 2006, **101**, 514–525.
3 A. Andersson, U. Rönner and P. E. Granum, What problems does the food industry have with the spore-forming pathogens *Bacillus cereus* and *Clostridium perfringens*?, *Int. J. Food Microbiol.*, 1995, **28**, 145–155.
4 A. Osimani, L. Aquilanti and F. Clementi, *Bacillus cereus* foodborne outbreaks in mass catering, *Int. J. Hosp. Manag.*, 2018, **72**, 145–153.
5 R. J. Manchee, M. G. Broster, I. S. Anderson, R. M. Henstridge and J. Melling, Decontamination of Bacillus anthracis on Gruinard Island?, *Nature*, 1983, **303**, 239–240.
6 A. Zhang, H. Sun, H. Xu, S. Qiu and X. Wang, Cell metabolomics, *OMICS*, 2013, **17**, 495–501.
7 J. Zhou, Q. Ma, H. Yi, L. Wang, H. Song and Y. J. Yuan, Metabolome profiling reveals metabolic cooperation between *Bacillus megaterium* and *Ketogulonicigenium vulgare* during induced swarm motility, *Appl. Environ. Microbiol.*, 2011, **77**, 7023–7030.
8 C. Laflamme, S. Lavigne, J. Ho and C. Duchaine, Assessment of bacterial endospore viability with fluorescent dyes, *J. Appl. Microbiol.*, 2004, **96**, 684–692.
9 B. Setlow, C. A. Loshon, P. C. Genest, A. E. Cowan, C. Setlow and P. Setlow, Mechanisms of killing spores of *Bacillus subtilis* by acid, alkali and ethanol, *J. Appl. Microbiol.*, 2002, **92**, 362–375.
10 W. Coleman, P. Zhang, Y.-q. Li and P. Setlow, Mechanism of killing of spores of Bacillus cereus and Bacillus megaterium by wet heat, *Lett. Appl. Microbiol.*, 2010, **50**, 507–514.
11 R. Rose, B. Setlow, A. Monroe, M. Mallozzi, A. Driks and P. Setlow, Comparison of the properties of *Bacillus subtilis* spores made in liquid or on agar plates, *J. Appl. Microbiol.*, 2007, **103**, 691–699.
12 A. C. Johansson, L. Landström, R. Öberg and P. O. Andersson, Monitoring deactivation processes of bacterial spores using fluorescence spectroscopy, in *Chemical, Biological, Radiological,*

Nuclear, and Explosives (CBRNE) Sensing XXIII, ed. J. A. Guicheteau and C. R. Howle, SPIE, 2022, p. 32.

13 K. L. Tyrrell, D. M. Citron, E. S. Leoncio, C. V. Merriam and E. J. Goldstein, Evaluation of cycloserine-cefoxitin fructose agar (CCFA), CCFA with horse blood and taurocholate, and cycloserine-cefoxitin mannitol broth with taurocholate and lysozyme for recovery of *Clostridium difficile* isolates from fecal samples, *J. Clin. Microbiol.*, 2013, **51**, 3094–3096.

14 I. Kirshenbaum, *Physical Properties of Heavy Water*, United States Atomic Energy Commission, Technical Information Division, 1948.

15 G. E. Walrafen, Raman spectral studies of water structure, *J. Chem. Phys.*, 1964, **40**, 3249–3256.

16 M. Zhang, W. Hong, N. S. Abutaleb, J. Li, P. T. Dong, C. Zong, P. Wang, M. N. Seleem and J. X. Cheng, Rapid Determination of Antimicrobial Susceptibility by Stimulated Raman Scattering Imaging of D_2O Metabolic Incorporation in a Single Bacterium, *Adv. Sci.*, 2020, **7**, 1–14.

17 D. Berry, E. Mader, T. K. Lee, D. Woebken, Y. Wang, D. Zhu, M. Palatinszky, A. Schintlmeister, M. C. Schmid, B. T. Hanson, N. Shterzer, I. Mizrahi, I. Rauch, T. Decker, T. Bocklitz, J. Popp, C. M. Gibson, P. W. Fowler, W. E. Huang and M. Wagner, Tracking heavy water (D_2O) incorporation for identifying and sorting active microbial cells, *Proc. Natl. Acad. Sci. U. S. A.*, 2015, **112**, E194–E203.

18 K. Yang, H. Z. Li, X. Zhu, J. Q. Su, B. Ren, Y. G. Zhu and L. Cui, Rapid Antibiotic Susceptibility Testing of Pathogenic Bacteria Using Heavy-Water-Labeled Single-Cell Raman Spectroscopy in Clinical Samples, *Anal. Chem.*, 2019, **91**, 6296–6303.

19 Y. Liu, Y. Ma, L. Zhang, X. Sun, J. Yang, X. Li, F. Li, R. Chen, P. Zhu, J. Xu and F. Yang, Single-cell Raman microspectroscopy-based assessment of three intracanal disinfectants' effect on *Enterococcus faecalis*, *J. Raman Spectrosc.*, 2022, **53**, 902–910.

20 S. A. Eichorst, F. Strasser, T. Woyke, A. Schintlmeister, M. Wagner and D. Woebken, Advancements in the application of NanoSIMS and Raman microspectroscopy to investigate the activity of microbial cells in soils, *FEMS Microbiol. Ecol.*, 2015, **91**, 1–14.

21 Y. Wang, Y. Song, Y. Tao, H. Muhamadali, R. Goodacre, N. Y. Zhou, G. M. Preston, J. Xu and W. E. Huang, Reverse and Multiple Stable Isotope Probing to Study Bacterial Metabolism and Interactions at the Single Cell Level, *Anal. Chem.*, 2016, **88**, 9443–9450.

22 M. Hekmatara, M. Heidari Baladehi, Y. Ji and J. Xu, D_2O-Probed Raman Microspectroscopy Distinguishes the Metabolic Dynamics of Macromolecules in Organellar Anticancer Drug Response, *Anal. Chem.*, 2021, **93**, 2125–2134.

23 W. Lester Jr., S. H. Sun and A. Seber, Observations on the influence of deuterium on bacterial growth, *Ann. N. Y. Acad. Sci.*, 1960, **84**, 667–677.

24 T. Stangner, T. Dahlberg, P. Svenmarker, J. Zakrisson, K. Wiklund, L. B. Oddershede and M. Andersson, Cooke–Triplet tweezers: more compact, robust, and efficient optical tweezers, *Opt. Lett.*, 2018, **43**, 1990.

25 T. Dahlberg, D. Malyshev, P. O. Andersson and M. Andersson, Biophysical fingerprinting of single bacterial spores using laser Raman optical tweezers, in *Chemical, Biological, Radiological, Nuclear, and Explosives (CBRNE) Sensing XXI, Chemical, Biological, Radiological, Nuclear, and Explosives (CBRNE)*, ed. J. A. Guicheteau and C. R. Howle, SPIE, 2020, p. 28.

26 D. Malyshev, R. Öberg, T. Dahlberg, K. Wiklund, L. Landström, P. O. Andersson and M. Andersson, Laser induced degradation of bacterial spores during micro-Raman spectroscopy, *Spectrochim. Acta, Part A*, 2022, **265**, 120381.

27 D. Malyshev, N. F. Robinson, R. Öberg, T. Dahlberg and M. Andersson, Reactive oxygen species generated by infrared laser light in optical tweezers inhibits the germination of bacterial spores, *J. Biophotonics*, 2022, **15**, 1–7.

28 Vibrational spectroscopy core facility, Umeå Unversity, accessed 22-10-04, 2022. URL: **https://www.umu.se/en/research/infrastructure/visp/downloads/**.

29 P. H. C. Eilers, Parametric Time Warping, *Anal. Chem.*, 2004, **76**, 404–411.

30 M. J. E. Savitzky and A. Golay, Smoothing and Differentiation, *Anal. Chem.*, 1964, **36**, 1627–1639.

31 M. Yasuda, N. Takeshita and S. Shigeto, Deuterium-labeled Raman tracking of glucose accumulation and protein metabolic dynamics in Aspergillus nidulans hyphal tips, *Sci. Rep.*, 2021, **11**, 1279.

32 X. Yuan and R. A. Mayanovic, An Empirical Study on Raman Peak Fitting and Its Application to Raman Quantitative Research, *Appl. Spectrosc.*, 2017, **71**, 2325–2338.

33 K. Palmö, B. Mannfors and L.-O. Pietilä, A comparison of methods for decomposing overlapping bands in Raman spectra, *J. Mol. Struct.*, 1988, **174**, 101–106.

34 S. B. Young and P. Setlow, Mechanisms of killing of *Bacillus subtilis* spores by hypochlorite and chlorine dioxide, *J. Appl. Microbiol.*, 2003, **95**, 54–67.

35 F. Janssen, A. Lund and L. Anderson, Colorimetric Assay for Dipicolinic Acid in Bacterial Spores Evidence for a New Growth-Promoting Acid Produced by *Lactobacillus casei*, *Science*, 1957, **127**, 5–6.

36 A. D. Warth, Heat stability of *Bacillus cereus* enzymes within spores and in extracts, *J. Bacteriol.*, 1980, **143**, 27–34.

37 T. Hamouda, A. Y. Shih and J. R. Baker, A rapid staining technique for the detection of the initiation of germination of bacterial spores, *Lett. Appl. Microbiol.*, 2002, **34**, 86–90.

38 J. Zhang, K. K. Griffiths, A. Cowan, P. Setlow and J. Yu, Expression Level of Bacillus subtilis Germinant Receptors Determines the Average Rate but Not the Heterogeneity of Spore Germination, *J. Bacteriol.*, 2013, **195**, 1735–1740.

39 L. Sinai, A. Rosenberg, Y. Smith, E. Segev and S. Ben-Yehuda, The molecular timeline of a reviving bacterial spore, *Mol. Cell*, 2015, **57**, 695–707. arXiv:arXiv:1011.1669v3.

40 T. Pirali, M. Serafini, S. Cargnin and A. A. Genazzani, Applications of Deuterium in Medicinal Chemistry, *J. Med. Chem.*, 2019, **62**, 5276–5297.